PROCEEDINGS OF SCIENCE

Next-generation LGADs: a measurement-simulation synergy to quantify donor removal

A. Fondacci,[a,b,*] **T. Croci,**[b] **A. R. Altamura,**[e] **R. Arcidiacono,**[d,e] **M. Boscardin,**[f] **N. Cartiglia,**[e] **M. Centis Vignali,**[f] **M. Ferrero,**[e] **A. Morozzi,**[b] **D. Passeri,**[c,b] **G. Paternoster,**[f] **B. Regnery,**[g] **V. Sola,**[h,e] **R. S. White**[e] **and F. Moscatelli**[i,b]

[a] *Dipartimento di Fisica, Università degli Studi di Perugia, Via Alessandro Pascoli, 06123 Perugia, Italy*
[b] *Istituto Nazionale di Fisica Nucleare (INFN) - Sezione di Perugia, Via Alessandro Pascoli, 06123 Perugia, Italy*
[c] *Dipartimento di Ingegneria, Università degli Studi di Perugia, Via Goffredo Duranti, 93, 06125 Perugia, Italy*
[d] *Dipartimento di Scienze del Farmaco, Università del Piemonte Orientale, Largo Donegani, 2, 28100 Novara, Italy*
[e] *Istituto Nazionale di Fisica Nucleare (INFN) - Sezione di Torino, Via Pietro Giuria, 1, 10125 Torino, Italy*
[f] *Fondazione Bruno Kessler (FBK), Via Sommarive, 18, 38123 Trento, Italy*
[g] *Karlsruhe Institute of Technology, Karlsruhe, Germany*
[h] *Dipartimento di Fisica, Università degli Studi di Torino, Via Pietro Giuria, 1, 10125 Torino, Italy*
[i] *Istituto Officina dei Materiali (IOM) CNR - Sede di Perugia, Via Alessandro Pascoli, 06123 Perugia, Italy*

E-mail: alessandro.fondacci@pg.infn.it

Recent advancements in Low-Gain Avalanche Diode (LGAD) architectures, including resistive and compensated designs, highlight the need for a precise understanding of donor removal at high donor concentrations to optimize their performance after irradiation. A method based on the variation of sheet resistance with fluence, measured through van der Pauw test structures, has been introduced to extract doping-removal coefficients. This approach was applied to resistive LGAD samples to quantify donor removal in the donor-doped resistive collection layer (NPLUS). Test structures from the RSD2 batch, manufactured by Fondazione Bruno Kessler with varying NPLUS doses, were irradiated up to 5.0×10^{15} 1 MeV n_{eq}/cm^2 at the JSI TRIGA reactor, and donor removal coefficients were experimentally determined using this method. In this contribution, TCAD simulations are used to validate the experimental results and to confirm the reliability of the van der Pauw-based extraction method.

33rd International Workshop on Vertex Detectors (VERTEX2025)
25-29 August 2025
University of Tennessee, Knoxville, USA

*Speaker

 ISSN 1824-8039 . Published by SISSA Medialab.

PoS(VERTEX2025)023

Contents

1. Introduction

Low-Gain Avalanche Diodes (LGADs) [1] achieve timing resolutions of several tens of picoseconds [2] up to fluences of about $2.5 \cdot 10^{15}$ 1 MeV n_{eq}/cm^2 [3], thanks to their internal signal amplification. LGADs will therefore be used in 1.3×1.3 mm^2 pixel arrays within the endcap timing layers of ATLAS [4] and CMS [5] for the High-Luminosity LHC upgrades to mitigate the high pile-up ($\sim$ 200). Their limitation in radiation tolerance is due to the acceptor-removal mechanism [6], i.e. the transformation of electrically active acceptor atoms into complex neutral defects, since internal signal amplification is achieved by an additional acceptor-type implant near the collecting electrode, which locally increases the electric field above the avalanche multiplication threshold. As a result, much research has focused on characterising acceptor removal [7].

Building on the excellent LGAD timing resolution, new LGAD architectures are being developed to meet the requirements demanded by future colliders [8], such as the Future Circular Collider (FCC). For future lepton colliders, resistive LGADs [9] are in development. They use a resistive collecting layer that acts as a current divider, enabling signal sharing among electrodes and reducing electrode density and power consumption. Internal signal amplification also allows for the use of thinner substrates, which reduces the material budget. For future hadron colliders, compensated LGADs [10] are being designed to extend radiation tolerance beyond 10^{17} 1 MeV n_{eq}/cm^2. In these devices, the gain implant is achieved through the compensation of acceptor and donor implants. Although both types of implants are gradually deactivated by irradiation, careful engineering aims to keep an active gain implant at extreme fluences, similar to new devices, thus preserving timing resolution comparable to unirradiated sensors.

In these advanced LGAD designs, donor implants play a role as significant as the acceptor gain implant in standard LGADs. In resistive LGADs, the resistive layer is donor-type, whereas in compensated LGADs, the gain implant is made through the compensation of acceptor and donor implants. Therefore, it is important to study donor removal at higher initial donor concentrations ($> 10^{16}$ at/cm^3) than those used in conventional n-type substrates [11]. Recently, the variation of sheet resistance with irradiation has been studied as a figure of merit for determining both acceptor and donor removal [12]. This method has already been applied to study donor removal in resistive LGADs with AC-coupled electrodes (AC-LGADs) [13]. The present work aims to validate these experimental findings by comparing them with TCAD simulations and thereby confirming the reliability of this approach.

2. Experimental determination of donor removal

As anticipated, donor removal in the resistive collection layer of the AC-LGAD, known as NPLUS in the Fondazione Bruno Kessler (FBK) terminology, was investigated by analyzing changes in sheet resistance following irradiation. Van der Pauw test structures from the RSD2 batch, produced by FBK and featuring different NPLUS doses (0.25, 0.50, and 1.00 in FBK's normalized units), were irradiated with neutrons at the JSI TRIGA reactor at fluence points of 1.0, 2.0, 3.5, and 5.0×10^{15} 1 MeV n_{eq}/cm^2.

Sheet resistance measurements were conducted before and after irradiation at room temperature in both Perugia and Karlsruhe to ensure reproducibility. A known current ramp was applied between two neighboring electrodes, and the voltage drop across the other two electrodes was recorded. Sheet resistance was calculated as the slope of the voltage-current plot multiplied by $\frac{\pi}{ln(2)}$. The current ramp ranged from -200 μA to +200 μA to maintain the voltage difference between the voltmetric electrodes within 1–100 mV. Voltage differences below this range make not negiglible parasitic contributions from the cables, while higher values may heat the sample and affect the measured sheet resistance. The van der Pauw test structures lack a contact on the back, so the probe station chuck was left floating, and four needles were used: two for current application and two for voltage measurement. Measurement results are presented in Figure 1 as sheet conductance, defined as the inverse of sheet resistance.

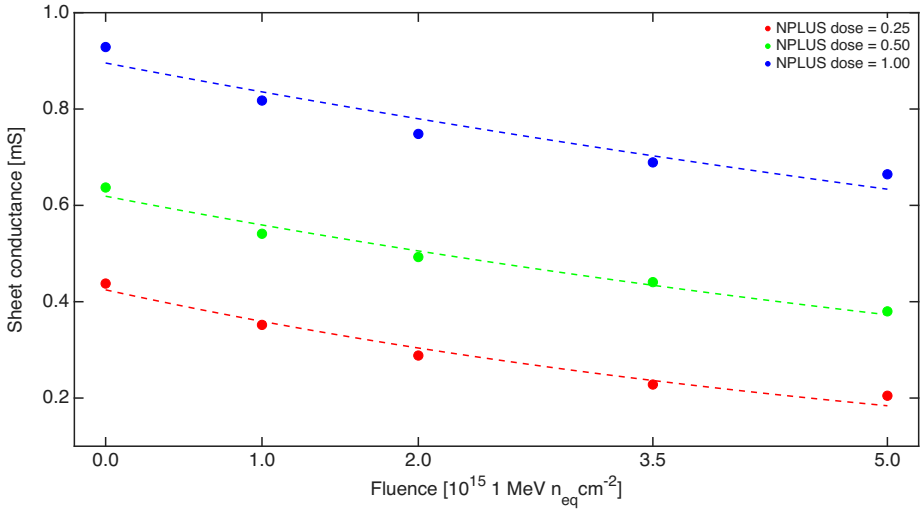

Figure 1: Markers indicate the experimental sheet conductances of the three different NPLUS implants, distinguished by color, measured using van der Pauw test structures irradiated with neutrons at the JSI TRIGA reactor at fluence points of 1.0, 2.0, 3.5, and 5.0×10^{15} 1 MeV n_{eq}/cm^2. Dashed lines represent the exponential fits used to extract the donor removal coefficients.

Donor removal, i.e. the deactivation of electrically active donor atoms into complex neutral defects, can be parametrised as [14]

$$N_D(\phi) = N_D(0) \cdot e^{-c_D \cdot \phi} \tag{1}$$

where ϕ represents the irradiation fluence in 1 MeV n_{eq}/cm^2, $N_D(\phi)$ and $N_D(0)$ denote the donor concentration after fluence ϕ and before irradiation, respectively, and c_D is the donor removal

coefficient. The latter has been extracted by fitting the sheet-conductance measurements to an exponential function and Figure 1 presents both the measurements and the corresponding exponential fits. The extracted donor removal coefficients are 1.5 ± 0.2, 1.0 ± 0.2, and $0.6 \pm 0.2 \times 10^{-16}$ cm^2 for NPLUS dose of 0.25, 0.50, and 1.00, respectively.

3. TCAD-based verification of donor removal

In this section, the experimentally extracted donor removal coefficients are validated using Synopsys Sentaurus Technology CAD (TCAD) simulations. Therefore, process simulations calibrated using Secondary-Ion Mass Spectrometry (SIMS) were conducted for the three different NPLUS doses (Figure 2a), and the resulting profiles were verified to reproduce the experimental sheet resistance measurements before irradiation. Within the simulation framework, sheet resistance was calculated using an analytical function implemented in TCAD. Indeed the simulation provides access to microscopic quantities, such as electron and hole concentrations and mobilities, enabling calculation of sheet resistance using the formula:

$$R_{sh} = \frac{1}{\int_0^d q[n(x)\mu_n(x) + p(x)\mu_p(x)]\,dx} \tag{2}$$

where q is the elementary charge, n and p are the electron and hole densities, μ_n and μ_p are the electron and hole mobilities, and d is the junction depth. This built-in function is applicable only

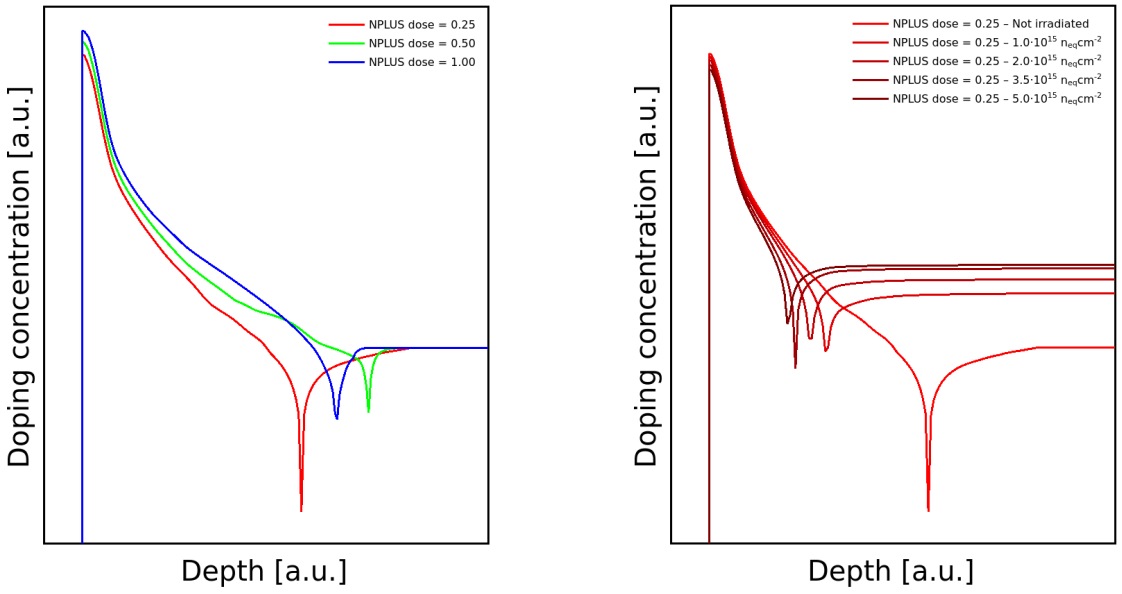

(a) All NPLUS not irradiated

(b) NPLUS dose = 0.25 at different fluences

Figure 2: **(a)** Process simulations calibrated using Secondary-Ion Mass Spectrometry (SIMS) data, for the three different NPLUS doses (0.25, 0.50, and 1.00 in FBK's normalized units). **(b)** NPLUS profile variation with irradiation for the lowest dose. The NPLUS is reduced according to equation 1, using the experimentally extracted $c_D = 1.5 \times 10^{-16}$ cm^2. The substrate doping concentration increases following the acceptor creation parameterization [7].

when the implant under test is of opposite doping type to the substrate of the van der Pauw test structure, as the junction depth cannot be defined otherwise. In this study, the NPLUS is a donor-doped implant, and the substrate is acceptor-doped. When the implant and substrate share the same doping type, a van der Pauw test structure must be reproduced in the 3D simulation environment, and sheet resistance is extracted following the previously outlined measurement procedure. This scenario is detailed in [12], which examines van der Pauw test structures of an acceptor implant on an acceptor substrate. The 3D van der Pauw test structure is necessary in this context to simulate the parasitic contribution from the substrate, as the implant and substrate are not separated by a depletion region formed across a pn junction.

Once the process simulations were confirmed to reproduce the sheet resistances of the three NPLUS implants before irradiation, the next step was to see if the experimental variations in sheet resistance after irradiation could be reproduced in simulation using the extracted donor removal coefficients. The Perugia radiation damage model [15], implemented in the TCAD framework, accounted for radiation damage effects via effective traps in the substrate and at the silicon-silicon oxide interface, as well as through analytical parameterizations that describe doping variation with irradiation. Figure 2b shows the simulated change in doping profile after irradiation for samples with the lowest NPLUS dose. Substrate doping concentration increased based on acceptor-creation parameterization [7], while NPLUS doping was reduced accordingly to equation 1 using experimentally extracted donor-removal coefficients. For example, a c_D value of $1.5 \cdot 10^{-16}$ cm^2 was used to reduce the NPLUS in Figure 2b. Post-irradiation sheet resistance was again calculated with the TCAD built-in function. Figure 3 compares simulation results (empty circles) and experimental measurements (filled markers of various shapes).

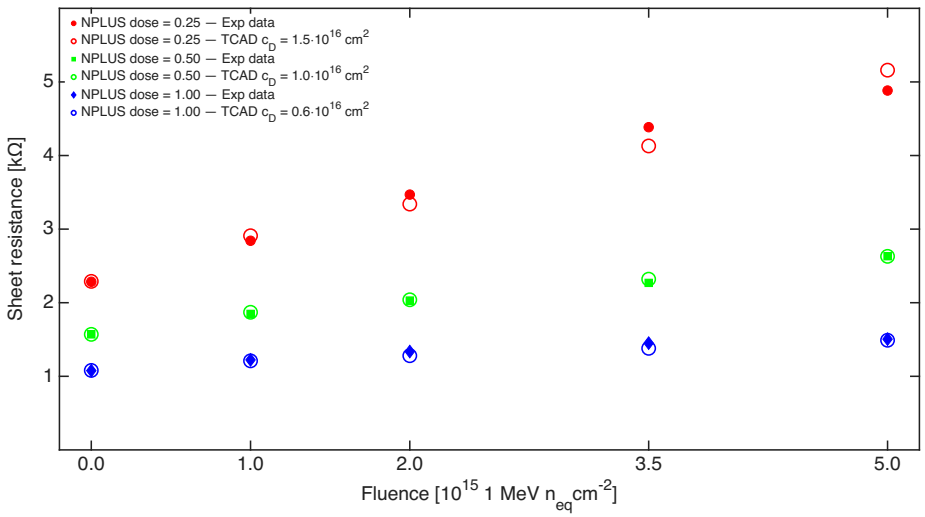

Figure 3: Comparison of sheet resistance measurements and simulations across varying fluences for three NPLUS doses: 0.25 (red), 0.50 (green), and 1.00 (blue). Measurements are shown as distinct filled markers, while simulations use open circle markers.

4. Conclusion

Emerging LGAD architectures, such as resistive LGADs and compensated LGADs, are being developed to meet the requirements of future colliders. In these devices, donor-type implants are as critical as the acceptor gain implant in standard LGADs. In resistive LGADs, the donor-doped resistive collection layer enables high spatial resolution (a few micrometres) even with large pixel sizes, thereby reducing channel density and power consumption. In compensated LGADs, potential frontrunners for 4D tracking (i.e., space plus time) at fluences exceeding 10^{17} 1 MeV n_{eq}/cm^2, the gain implant is achieved through precisely balanced compensation of acceptor and donor doping.

Characterising donor removal at higher initial donor concentrations than those used in conventional n-type substrates is essential for optimising these new LGAD architectures. A novel investigation technique has been introduced. It examines the variation in sheet resistance, measured using van der Pauw test structures, under irradiation to extract the doping-removal coefficient. This methodology has been applied to study donor removal in the resistive collection layer (NPLUS) of resistive LGADs. Samples from the RSD2 batch, featuring three different NPLUS doses, were used. In this contribution, the experimentally extracted donor removal coefficients were validated through comparison with TCAD simulations. Process simulations calibrated on SIMS data for the three NPLUS doses were produced and scaled with irradiation using the experimentally determined donor removal coefficients. Additionally, the Perugia radiation damage model was implemented in TCAD to account for radiation damage effects. A built-in analytical function was used to extract the simulated sheet resistance.

The observed agreement between measurements and simulations across varying fluence values validates the doping removal extraction method using van der Pauw test structures. Therefore, for doping profiles with maximum concentration near the silicon-silicon oxide interface, and where the substrate of the van der Pauw test structure is of the opposite doping type, as in the examined NPLUS case, fitting the variation of sheet conductance with irradiation using an exponential function enables the extraction of the doping removal coefficient for the implant, whether acceptor or donor type.

Acknowledgments

This work has received funding from the European Union's Horizon 2020 Europe research and innovation program under grant agreement No 654168 'AIDA-2020', the PRIN MIUR project 2017L2XKTJ '4DInSiDe', and the European Union. Views and opinions expressed are however those of the authors only and do not necessarily reflect those of the European Union or the European Research Council Executive Agency. Neither the European Union nor the granting authority can be held responsible for them. This work is supported by ERC grants (UFSD, 669529 and CompleX, 101124288).

References

[1] G. Pellegrini et al., *Technology developments and first measurements of Low Gain Avalanche Detectors (LGAD) for high energy physics applications*, *Nucl. Instrum. Meth. A* **765** (2014) 12.

[2] N. Cartiglia et al., *Beam test results of a 16ps timing system based on ultra-fast silicon detectors*, *Nucl. Instrum. Meth. A* **850** (2017) 83.

[3] R.S. White et al., *Characterisation of the FBK EXFLU1 thin sensors with gain in a high fluence environment*, *Nucl. Instrum. Meth. A* **1068** (2024) 169798.

[4] ATLAS collaboration, *Technical Proposal: A High-Granularity Timing Detector for the ATLAS Phase-II Upgrade*, Tech. Rep. , CERN, Geneva (2018), DOI.

[5] CMS collaboration, *Technical proposal for a MIP timing detector in the CMS experiment Phase 2 upgrade*, Tech. Rep. , CERN, Geneva (2017), DOI.

[6] G. Kramberger et al., *Radiation effects in Low Gain Avalanche Detectors after hadron irradiations*, *JINST* **10** (2015) .

[7] M. Ferrero et al., *Radiation resistant LGAD design*, *Nucl. Instrum. Meth. A* **919** (2019) 16.

[8] ECFA Detector R&D Roadmap Process Group, *The 2021 ECFA detector research and development roadmap*, Tech. Rep. Geneva (2020), DOI.

[9] M. Tornago et al., *Resistive AC-Coupled Silicon Detectors: Principles of operation and first results from a combined analysis of beam test and laser data*, *Nucl. Instrum. Meth. A* **1003** (2021) 165319.

[10] V. Sola et al., *A compensated design of the LGAD gain layer*, *Nucl. Instrum. Meth. A* **1040** (2022) 167232.

[11] R. Wunstorf et al., *Investigations of donor and acceptor removal and long term annealing in silicon with different boron/phosphorus ratios*, *Nucl. Instrum. Meth. A* **377** (1996) 228.

[12] A. Fondacci et al., *Compensated LGAD optimisation through van der Pauw test structures*, *Nucl. Instrum. Meth. A* **1080** (2025) 170800.

[13] U. Elicabuk et al., *Irradiation studies of the Resistive AC-coupled Silicon Detector (RSD/AC-LGAD)*, *Nucl. Instrum. Meth. A* **1080** (2025) 170705.

[14] M. Moll et al., *Investigation on the improved radiation hardness of silicon detectors with high oxygen concentration*, *Nucl. Instrum. Meth. A* **439** (2000) 282.

[15] A. Morozzi et al., *TCAD simulations for radiation-tolerant silicon sensors*, *PoS* **VERTEX2023** (2024) 060.